Multispectral Imaging of T and B Cells in Murine Spleen and Tumor

Zipei Feng,*,† Shawn M. Jensen,* David J. Messenheimer,*,‡ Mohammed Farhad,*,† Michael Neuberger,*,[1] Carlo B. Bifulco,§ and Bernard A. Fox*,‡

Recent advances in multiplex immunohistochemistry techniques allow for quantitative, spatial identification of multiple immune parameters for enhanced diagnostic and prognostic insight. However, applying such techniques to murine fixed tissues, particularly sensitive epitopes, such as CD4, CD8α, and CD19, has been difficult. We compared different fixation protocols and Ag-retrieval techniques and validated the use of multiplex immunohistochemistry for detection of $CD3^+CD4^+$ and $CD3^+CD8^+$ T cell subsets in murine spleen and tumor. This allows for enumeration of these T cell subsets within immune environments, as well as the study of their spatial distribution. ***The Journal of Immunology*****, 2016, 196: 3943–3950.**

Assessment of patterns of immune infiltrates was shown to be highly prognostic and diagnostic in many types of cancers (1, 2). The clinical impact of such analysis is most notably shown in colon cancer, where objective quantification of $CD3^+$ and $CD8^+$ T cell densities in the primary tumor has a highly significant impact on patient prognosis (3). More recently, multiplex immunohistochemistry (IHC) has emerged as a powerful technique for the study of multiple immune parameters on a single slide. This increases efficiency and, more importantly, allows for the study of relationships between cell populations, offering greater insight into the mechanisms underlying various disease processes (4).

Multiplex IHC platforms have been used with human tissues, but their use with murine fixed tissues is still being optimized. Many Abs against human Ags are successfully used with paraffin sections for human IHC, but considerably fewer are available for mouse Ags. Notably, there has been a dilemma in the field about performing IHC staining on certain immune epitopes, such as CD4, CD8α, and CD19, which stain functionally distinct T and B cell populations. These fixation-sensitive epitopes are not easily detected in formalin-fixed–paraffin-embedded (FFPE) tissues and historically have relied on frozen tissue for detection; however, this comes at the expense of the integrity of tissue architecture, making it difficult to study tissue morphology (5–8). Although it was suggested that zinc-based fixation buffers are superior for preserving these epitopes compared with formalin fixation (9, 10), the specificity of the Abs and the ability to multiplex under these conditions have not been tested. Being able to perform CD4 and CD8 staining reliably in paraffin-embedded murine tissues is critical to our understanding of their function in various physiological and disease processes, especially given that certain immune cell subtypes, such as tissue-resident memory T cells, were reported to be underestimated using standard flow cytometry techniques (11). In our study, we compared multiple fixation protocols, as well as Ag-retrieval methods, to validate the use of multiplex IHC in murine tissues with sensitive epitopes, such as CD4, CD8α, and CD19. Our approach allows for successful detection and quantification of five or more markers on murine tissues.

Materials and Methods

Mice

Female C57BL/6 mice, $Rag1^{-/-}$ mice (B6.129S7-$Rag1^{tm1Mom}$/J), pmel-1 TCR-transgenic mice [B6.Cg-*Thy1*^{a}/Cy Tg(TcraTcrb)8Rest/J], and TRP1 TCR/$Rag1^{-/-}$-transgenic mice [B6.Cg-*Rag1*^{tm1Mom} *Tyrp1*$^{B\text{-}w}$*Tg*(*Tcra,Tcrb*)*9Rest/J*] were purchased from The Jackson Laboratory (Bar Harbor, ME). pmel-1 TCR-transgenic mice were bred to $Rag1^{-/-}$ mice to generate pmel TCR/$Rag1^{-/-}$ mice. pmel TCR/$Rag1^{-/-}$ mice have $CD8^+$ T cells expressing a transgenic TCR specific for $mgp100_{(25–33)}$ peptide. TRP1 TCR/$Rag1^{-/-}$-transgenic mice have $CD4^+$ T cells expressing a transgenic TCR specific for $mtyrp1_{(113–127)}$ peptide. All mice were maintained in a specific pathogen–free environment. Recognized principles of laboratory animal care were followed (*Guide for the Care and Use of Laboratory Animals*, National Research Council, 2011), and all animal protocols were approved by the Earle A. Chiles Research Institute Animal Care and Use Committee.

Tumor cell lines

The sarcoma cell line MCA-310 (12) and the squamous cell carcinoma cell line SCCVII (13) were maintained in complete media. For MCA-310, 20,000 cells were injected s.c. into the flank of C57BL/6 mice, whereas for SCCVII, 1 million cells were injected s.c. into the back of the neck of C3H/HeJ mice. Mice were sacrificed, and the established tumors were resected, fixed in zinc fixation buffer, and processed with a Tissue-Tek automated tissue processor.

Immunohistochemistry

Tissue fixation and processing. One liter of zinc-fixation buffer was prepared by mixing 0.5 g calcium acetate (402850), 5 g zinc acetate (Z0625),

*Robert W. Franz Cancer Research Center, Earle A. Chiles Research Institute, Providence Cancer Center, Providence Portland Medical Center, Portland, OR 97213; †Department of Cell, Developmental & Cancer Biology, Oregon Health & Science University, Portland, OR 97239; ‡Department of Molecular Microbiology & Immunology, Oregon Health & Science University, Portland, OR 97239; and §Department of Pathology, Providence Portland Medical Center, Portland, OR 97213

[1]Current address: Department of General, Visceral, Transplantation, Vascular, and Thoracic Surgery, Hospital of the Ludwig Maximilian University, Munich, Germany.

ORCIDs: 0000-0003-1396-9227 (Z.F.); 0000-0002-4843-5930 (S.M.J.); 0000-0002-3512-7509 (M.F.); 0000-0001-8453-5325 (M.N.); 0000-0002-4452-5947 (B.A.F.).

Received for publication December 31, 2015. Accepted for publication February 22, 2016.

Address correspondence and reprint requests to Dr. Bernard A. Fox, Earle A. Chiles Research Institute, 4805 Northeast Glisan Street, Room 2N56, Portland, OR 97213. E-mail address: bernard.fox@providence.org

The online version of this article contains supplemental material.

Abbreviations used in this article: DC, dendritic cell; ddH_2O, double-distilled H_2O; FFPE, formalin-fixed–paraffin-embedded; IHC, immunohistochemistry; NBF, neutral-buffered 10% formalin; PLP, periodate–lysine–paraformaldehyde; RT, room temperature; TSA, tyramide; WT, wild-type.

and 5 g zinc chloride (208086) with 0.1 M Tris (251-018; all from Sigma) (pH 7.4). The final pH was 6.5–7.

Periodate–lysine–paraformaldehyde (PLP) was prepared by mixing Lysine HCl (L5626; Sigma) solution (13.7 g Lysine HCl in 375 ml double-distilled H_2O [ddH_2O] [adjust pH to 7.4] with Na_2HPO_4 [W239901; Sigma]) with 15.6 ml 16% paraformaldehyde (15712; Electron Microscopy Sciences). A total of 2.14 g sodium periodate (311448; Sigma) was added, and the solution was brought up to 1 l with 0.1 M phosphate buffer (W2399D1; Sigma).

Spleens and tumors were harvested and fixed for 24 h at room temperature (RT). Spleens and tumors were processed using a Tissue-Tek automated tissue processor (Sakura) on Zinc setting for zinc- and PLP-fixed samples (start on 70% ethanol, skip formalin fixation) and embedded with a Leica tissue embedder.

Four-micron-thick sections were cut and floated onto Plus slides (Cardinal Colorfrost) in a tissue flotation bath set at 40˚C (Fisher Healthcare). Slides were allowed to dry at RT overnight and stored at 4˚C until use.

Deparaffinization, staining, imaging, and analysis. Slides were placed on a staining rack in a Leica autostainer, and a deparaffinization protocol was run (70% ethanol 30 min, 95% ethanol 30 min two times, 100% ethanol 30 min three times, xylene 40 min two times, paraffin 35 min four times). Samples were marked with an ImmEdge Hydrophobic Barrier Pen (Vector) and allowed to dry. Slides were rinsed once with 1× TBST (10× solution: 88 g Trizma base, 24 g NaCl in 1 l ddH_2O [adjust pH to 7.6]) and blocked with Renaissance Ab diluent (PD905; Biocare Medical) for 10 min.

Primary Ab was diluted in Renaissance Ab diluent (PD905; Biocare Medical). The dilutions used were 1:50 for CD3 (SP7, M3074; Spring Bioscience), CD4 (RM4-5, 550280, BD Biosciences; GK1.5, 14-0041-85, eBioscience), CD8 (53-6.7, 550281; BD Biosciences), CD19 (1D3, 553783; BD Biosciences), and granzyme B (polyclonal rAB, ab4059; Abcam); 1:100 for Foxp3 (FJK-16s, 14-5773; eBioscience) and PD-L1 (ab58810; Abcam); and 1:250 for F4/80 (CI:A3-1, MCA497GA; AbD Serotec). Primary Abs were incubated for 45 min on an orbital shaker (SHKA2000; Thermo Scientific) at RT. Abs were subsequently removed by vacuum, and slides were washed three times for 30 s in TBST.

Anti-rabbit secondary Ab (87-9623; Life Technologies) or anti-rat (MP-7444-15; Vector Laboratories) was added drop-wise to slides to cover the tissue area. Slides were incubated for 10 min at RT and washed three times for 30 s in 1× TBST.

Tyramide (TSA)-conjugated fluorophore (NEL791001KT, PerkinElmer; T20950, Life Technologies) was added to slides at 1:100 dilution in Amplification plus buffer (NEL791001KT; PerkinElmer) and incubated for 10 min at RT; TSA was vacuumed off, and slides were washed three times for 30 s in 1× TBST.

For multiplex imaging, Ag-stripping buffer (0.1 M glycine [G2879; Sigma], adjust pH to 10 using NaOH [SS267; Fisher Chemical], 0.5% Tween) was added to slides and incubated for 10 min at RT. Slides were rinsed with TBST, blocked briefly, and incubated with primary Ab at the desired dilution and time. DAPI (D1306; Life Technologies, 1 mg/ml stock) was diluted 1:500 in TBST and added to slides. Slides were incubated for 5 min at RT and washed twice for 30 s in TBST. Slides were rinsed with ddH_2O, coverslipped with VECTASHIELD Hard Mount (Vector Laboratories), painted with nail polish (L.A. Colors), and stored at 4˚C in a covered slide box. Slides were imaged at 4× and 20× using Vectra imaging software, and the number of cells was enumerated from 20× fields using inForm analysis software (both from PerkinElmer).

Results

Murine CD3, CD4, and CD8 fluorescent IHC

Neutral-buffered 10% formalin (NBF) has been the standard for fixation for human tissues; it preserves tissue architecture and historically has been used for single color and multiplex IHC (5, 14). For murine tissues, NBF, when combined with standard heat-mediated Ag retrieval, is excellent for detecting immune markers, such as CD3; however, the use of NBF to fix mouse spleens resulted in an inability to detect CD4 and CD8α epitopes (Fig. 1). To address this problem, we examined two alternative fixation methods. PLP is a fixative that acts by cross-linking lysine residues; it was shown to be compatible with many epitopes for the use in IHC (15, 16). In murine spleen sections fixed with PLP, we

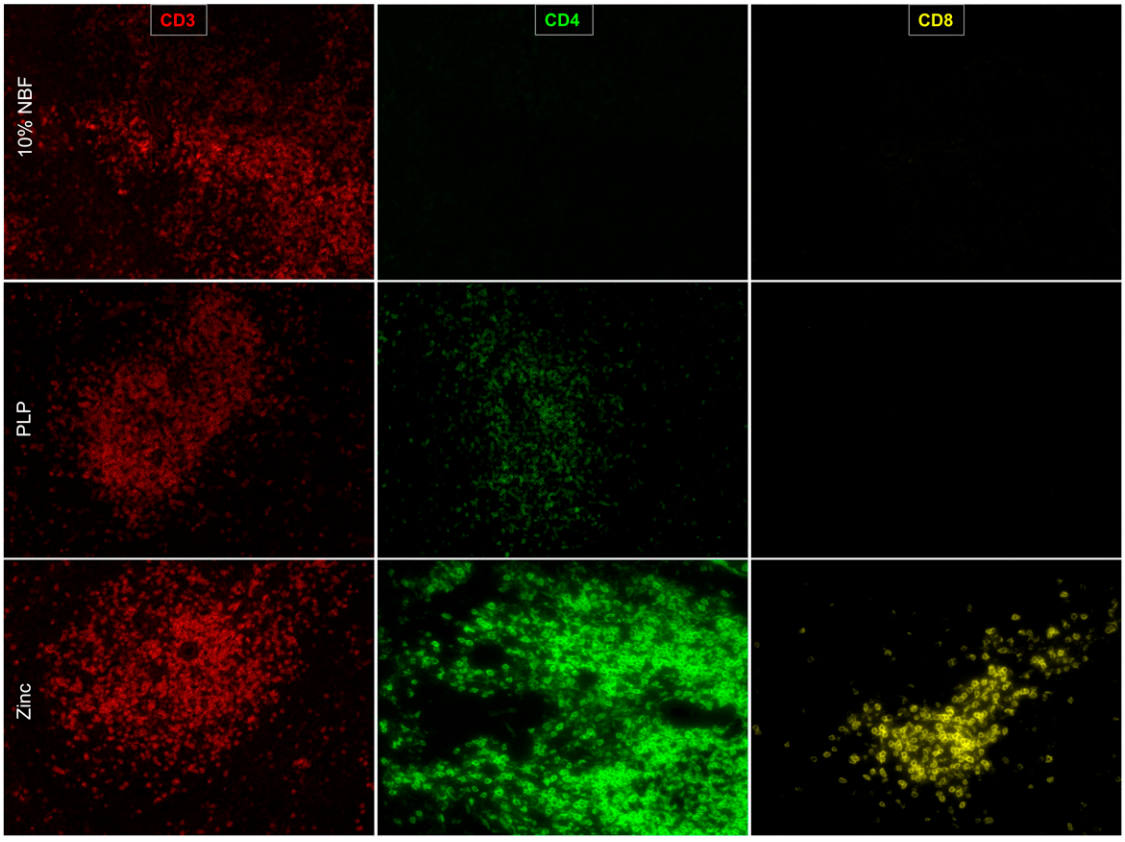

FIGURE 1. Zinc-based buffer is superior in detection of CD4 and CD8α. Spleen sections were fixed for 24 h in each condition and 4-μm sections were cut and prepared. Ag retrieval was performed on formalin-fixed tissues but not on PLP or zinc-fixed tissues. Tissue sections were imaged at 20× with a PerkinElmer Vectra platform.

were able to detect CD3 and CD4 epitopes; however, the intensity of CD4 staining was weak, and we were not able to detect CD8α (Fig. 1).

Traditionally, zinc-based fixation has been an additive to NBF for improved Ag preservation. However, reports have suggested that zinc-based fixative devoid of NBF could maintain Ag integrity without sacrificing much of the architecture (9, 10, 17). We did not notice a significant difference in tissue architecture between NBF and the zinc-based fixative (Supplemental Fig. 1A, 1B). Importantly, we found that spleen tissue fixed in the zinc-based fixation buffer was superior to both formalin-fixed or PLP-fixed tissue in detection of CD3, CD4, and CD8α epitopes (Fig. 1).

To validate the CD4 and CD8α staining, we obtained spleens from Rag1$^{-/-}$-transgenic mice, which lack T cells and B cells, as well as from a transgenic CD8^{+} TCR mouse that recognizes gp100 protein (pmel) and a transgenic CD4^{+} TCR mouse that recognizes

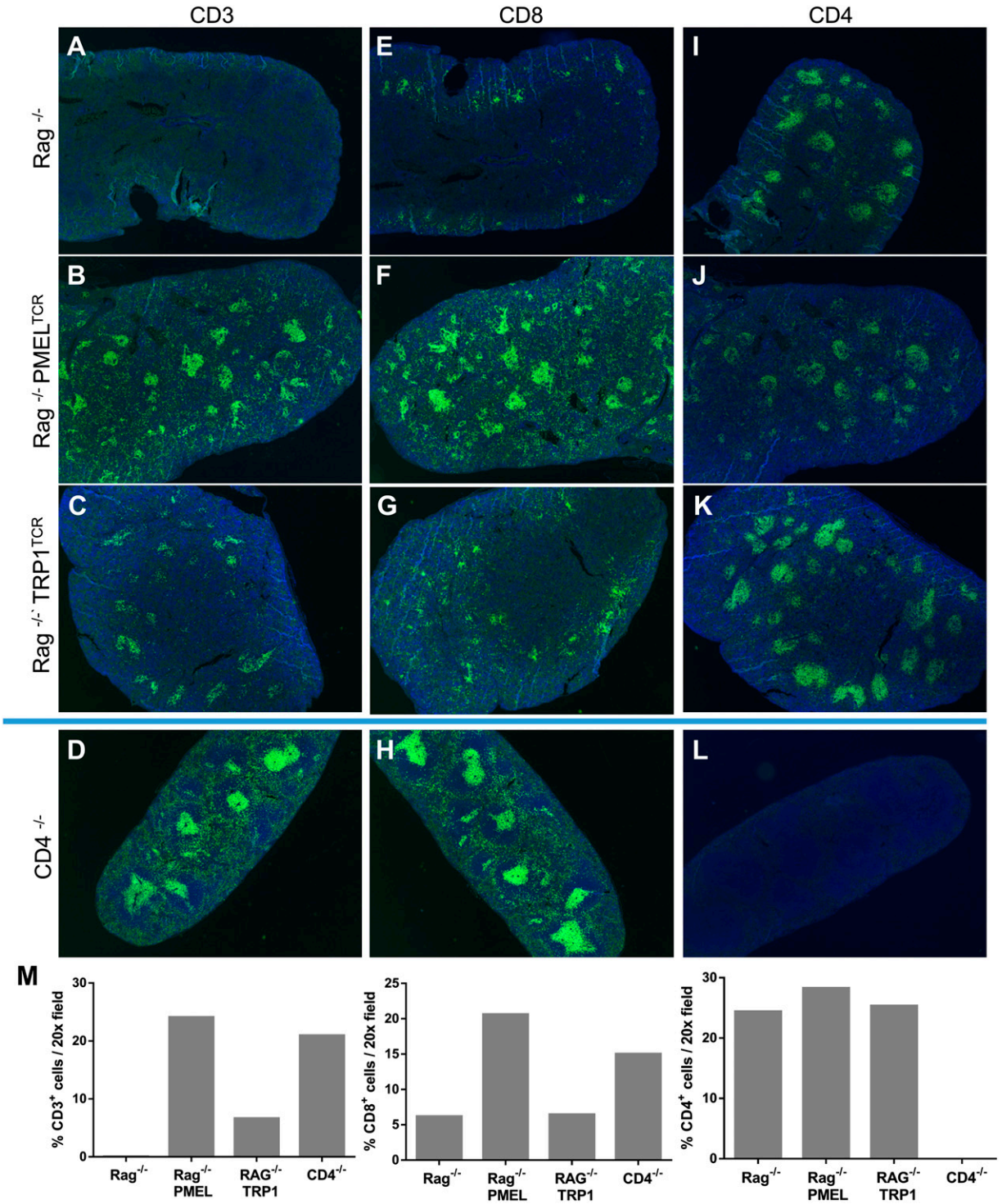

FIGURE 2. CD4 and CD8 staining in spleen sections. Spleens were fixed for 24 h for each condition. Single stains with CD3, CD4, or CD8 Ab were performed, and tissue sections were imaged at 4× with a PerkinElmer Vectra platform. Spleens from Rag1-knockout mice were stained for CD3 (**A**), CD8 (**E**), or CD4 (**I**). Stains were also performed on spleens from pmel TCR-transgenic (**B**, **F**, and **J**) or TRP1 TCR-transgenic (**C**, **G**, and **K**) mice, both on a Rag1-knockout background. Stains were also performed on CD4-knockout mice (**D**, **H**, and **L**). (**M**) Cells were enumerated as the percentage of positive cells in a 20× field.

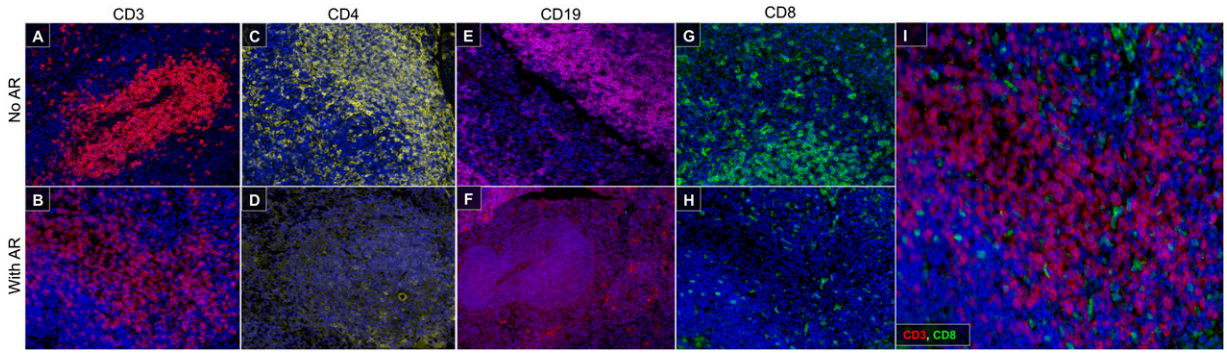

FIGURE 3. Heat-mediated Ag retrieval diminishes CD4, CD19, and CD8 staining. Heat-mediated Ag retrieval with Biogenex Citra buffer was performed using a microwave. Slides were microwaved for 25 s to bring to a boil on high power and maintained for 10 min on 10% power. Ab staining were performed with (**B**, **D**, **F**, and **H**) or without (**A**, **C**, **E**, and **G**) Ag retrieval. (**I**) Merge of CD3 and CD8 after Ag retrieval. Original magnification ×20.

tyrp1 protein (TRP1). Both of the TCR-transgenic mice were crossed to Rag1$^{-/-}$ mice to ensure that only transgenic T cells were present. Spleen sections were cut and stained with CD3, CD4, and CD8α Abs. As expected, CD3 staining was absent in Rag1$^{-/-}$ spleens, but the presence of CD3$^+$ cells was noted in pmel and TRP1 spleens (Fig. 2A–C, 2M). Interestingly, we observed the presence of a small population of cells that stained with CD8α in Rag1$^{-/-}$ mice; however, these CD8α$^+$ cells did not stain with CD3 (Fig. 2A, 2E). Based on their morphology and location within the spleen, they are most likely CD3$^-$CD8α$^+$ dendritic cells (DCs) (18). In pmel-transgenic animals, we saw an increase in CD3$^+$CD8α$^+$ cells (Fig. 2B, 2F, 2M), confirming the recognition of the Ab to CD8$^+$ T cells. We observed CD3$^-$CD4$^+$ cells in the spleens from Rag1$^{-/-}$ and Rag1$^{-/-}$ pmel TCR-transgenic mice (Fig. 2A, 2B, 2I, 2J). Rag1$^{-/-}$ TRP1 TCR-transgenic mice showed a small population of CD3-expressing cells in the T cell areas of the spleen (Fig. 2C); interestingly, this did not correlate with an increased expression of CD4 in these spleens compared with Rag1$^{-/-}$ or Rag1$^{-/-}$ pmel TCR-transgenic mice (Fig. 2I–K, 2M). Although CD4, like CD8α, can also be expressed in non-T cells, such as macrophages and DCs (19–21), we wanted to validate the specificity of the CD4 staining. To do this, we stained a spleen from a CD4$^{-/-}$ mouse. We did not observe any CD4 staining in the CD4$^{-/-}$ spleen, confirming the specificity of the Ab (Fig. 2D, 2H, 2L). The existence of these CD3$^-$CD4$^+$ cells highlights the importance of multiplex IHC, which allows us to separate the CD3$^+$CD4$^+$ T cells from the CD4$^+$ myeloid cells to accurately identify and study these distinct populations.

Murine multiplex fluorescent IHC

Our previous work showed that a TSA-based multiplex fluorescent imaging platform can be used to predict the success of culturing tumor-infiltrating lymphocytes from human melanoma samples (22). A simple diagram of this protocol is shown in Supplemental Fig. 2. Briefly, tissue sections were Ag retrieved, stained with primary and secondary Abs, and stained with TSA conjugated to a fluorochrome label. This was followed by heat-mediated Ag stripping to remove the primary Ab to label with a new primary Ab. To establish a multiplex protocol in murine samples, we tried heat-mediated Ag stripping on murine zinc-fixed tissues. We found that, after Ag retrieval, we were able to stain for CD3 (Fig. 3A, 3B), but we lost the ability to stain for CD4 (Fig. 3C, 3D) and CD19 (Fig. 3E, 3F). Although we saw CD8α staining on the tissue following Ag retrieval (Fig. 3G, 3H), these were not T cells, because none of the CD8α$^+$ cells costained with anti-CD3 (Fig. 3I). To circumvent this issue, we prepared and compared two non–heat-mediated glycine-based stripping buffers: basic (pH 10) and acidic (pH 2). Spleen tissue sections were sequentially stained with CD8α, CD4, and CD19 in that order, and Ag-stripping buffer was applied between Abs. We found that the basic Ag-stripping buffer (pH 10) was superior in maintaining subsequent CD4 and CD19 staining intensity (Fig. 4A) compared with the acidic stripping buffer (Fig. 4B). We subsequently tested the stripping efficiency using the basic stripping buffer. We found that the pH-10 buffer was able to sufficiently strip the previous Ab, allowing for subsequent staining with no cross-epitope staining (Fig. 4C–F). This demonstrates that the basic stripping buffer is suitable for multiplex fluorescent IHC detection of sensitive T and B cell markers in murine tissues. We were able to use the basic stripping buffer to successfully identify CD3, CD4, and CD8 populations in the spleen (Fig. 5A–G).

The presence of CD4 staining in Rag1$^{-/-}$ mice is interesting and collaborates other reports showing the presence of CD3$^-$CD4$^+$ DCs in murine tissues (19, 21). To determine whether these CD3$^-$CD4$^+$ cells are DCs, we stained for DC marker CD11c using our multiplex protocol and found that a significant portion of the CD4$^+$ cells expressed CD11c (Supplemental Fig. 3A–D). Using flow cytometry, we also determined that these CD3$^-$CD4$^+$ cells can express CD11b, consistent with previous reports that macrophages can express CD4 (23) (Supplemental Fig. 3E). We next wanted to address whether their residence in the follicles of the spleen of Rag1$^{-/-}$ mice would be displaced if CD3$^+$CD4$^+$, CD3$^+$CD8$^+$, and CD19$^+$ B cells were adoptively transferred into these mice. To do this, we adoptively transferred splenocytes from wild-type (WT) C57BL/6 mice into syngeneic Rag1$^{-/-}$-transgenic mice. Spleens from the receiving animal were harvested 14 d postadoptive transfer and assessed for the presence of T and B cells. We found that, following the adoptive transfer, there was a significant increase in CD19$^+$ B cells and CD3$^+$ T cells (Fig. 6F, 6I, 6L, 6N), with a concurrent decrease in CD3$^-$CD4$^+$ cells (Fig. 6K). Furthermore, the majority of CD19$^+$ B cells and CD3$^+$ T cells, as indicated by IHC, were located inside the follicles, surrounded by CD3$^-$CD4$^+$ cells (Fig. 6F–J). This suggests that the T and B cells adoptively transferred to the spleen of Rag1$^{-/-}$ mice preferentially migrate to the follicles and displace the CD3$^-$CD4$^+$ cells, which could mediate the development of T and B cells.

Finally, we wanted to evaluate whether this multiplex technique could be used to stain immune cells in a tumor setting. We injected C57BL/6 mice s.c. with a methylcholanthrene-induced sarcoma cell line. Tumors were harvested and stained for CD3, CD4, CD8, Foxp3, and F4/80 using our multiplex IHC protocol. We were able to identify distinct T cell populations in the tumor (Fig. 7) and separate them into CD3$^+$CD4$^-$CD8$^-$ T cells, CD3$^+$CD8$^+$ T cells, CD3$^+$CD4$^+$Foxp3$^-$ T cells, and CD3$^+$CD4$^+$Foxp3$^+$ regulatory

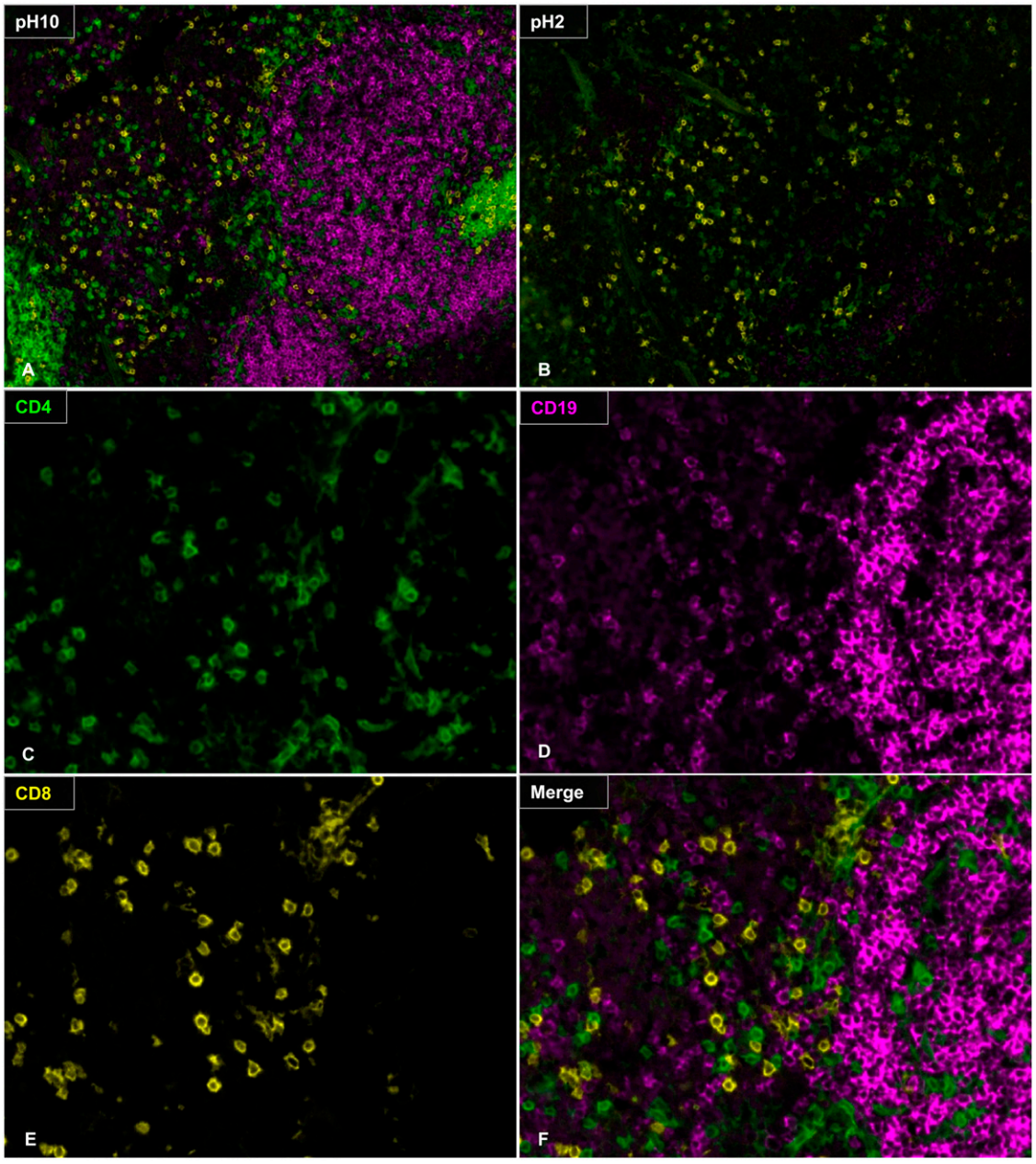

FIGURE 4. Multiplex IHC with CD4, CD8, and CD19. Slides were stained with CD8 (yellow) and exposed to Ag-stripping buffer (100 mM glycine, 0.5% Tween) of pH 10 (**A**) or pH 2 (**B**). Slides were stained for CD4 (green), followed by Ag stripping and CD19 staining (magenta). (**C**–**F**) Higher magnification of the slides stripped with pH-10 buffer. Original magnification ×20.

T cells. This multiplex IHC protocol was verified in a second murine tumor model with a spontaneously squamous cell carcinoma cell line (SCCVII).

Discussion

Immunohistochemical approaches on FFPE tissues have long been the standard for morphological analysis. More recently, quantitative IHC methods showed promise in the development of cancer diagnostics and prognostic biomarkers for tailored therapy (24, 25). This is especially useful in the era of immunotherapy because many immunotherapies can benefit from biomarkers, allowing for directed treatment. Methods such as multiplex IHC have been in the forefront of development because they significantly enrich the data extracted from the tissue microenvironment and allow for relationship analysis between cell subsets for added information. Much of the work has been done on human tissues as the staining of various epitopes on FFPE tissues has been optimized (4, 22). For murine studies, characterization of the immune distribution in the tissue by IHC is lacking because many epitopes, notably CD4 and CD8, are sensitive to cross-linking and are unable to be detected in FFPE samples. Frozen sections are sometimes used for these sensitive Abs (26), but this results in distorted tissue architecture and artifacts that compromise morphological studies. For these reasons, flow cytometry has long been the gold standard for analysis of immune infiltrates in the tumor microenvironment (27). However, flow cytometry does not provide sufficient contextual information, which was shown, in murine and human studies, to be important in understanding the biological basis of diseases and for predicting outcome in various types of cancer (1, 3). It was suggested that alternative fixation methods, such as PLP and zinc-based fixation, are superior to formalin in preserving certain epitopes, but the specificity of the Abs under these con-

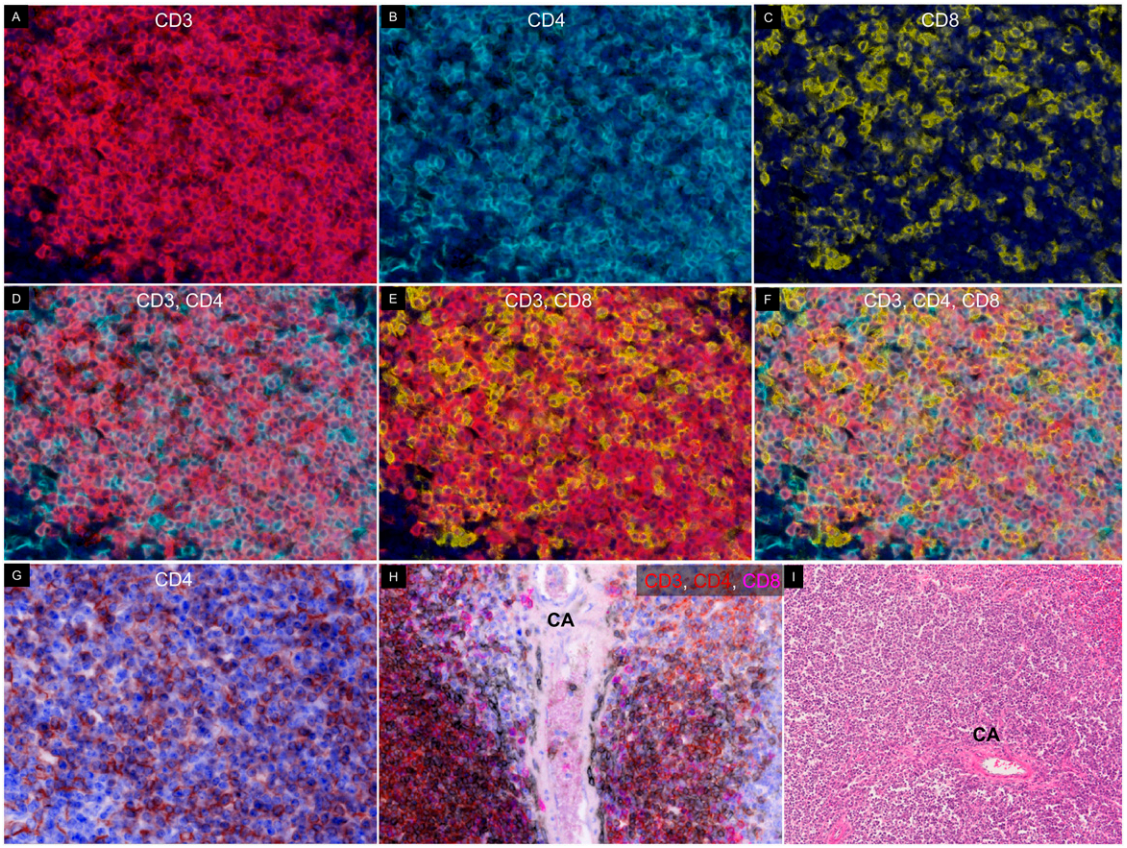

FIGURE 5. Staining of CD4 and CD8 T cells in spleen. Slides were stained with CD3 (**A**), CD4 (**B**), and CD8 (**C**) in that order with Ag stripping in between. (**D**) Merge of CD3 and CD4. (**E**) Merge of CD3 and CD8. (**F**) Merge of CD3, CD4, and CD8. (**G**) Pseudo-H&E image of CD4 staining with DAPI. (**H**) Pseudo-H&E image of CD3 (red), CD4 (brown), and CD8 (magenta) on cells adjacent to a central artery (CA). (**I**) H&E image of spleen sections showing lymphocyte distribution around a CA. Original magnification ×20.

ditions are not characterized, and their application in a multiplex platform is unknown. Our study showed that zinc-based fixation is superior to PLP and formalin for the detection of sensitive epitopes, such as CD4 and CD8 (Fig. 1), and it may be applied to a broader selection of Abs traditionally reserved for flow cytometry and frozen sections, such as CD19. These results were not unique to the chosen clones of mAbs; we also observed staining with a different clone targeting CD4 (RM4-5, Fig. 1; GK1.5, Supplemental

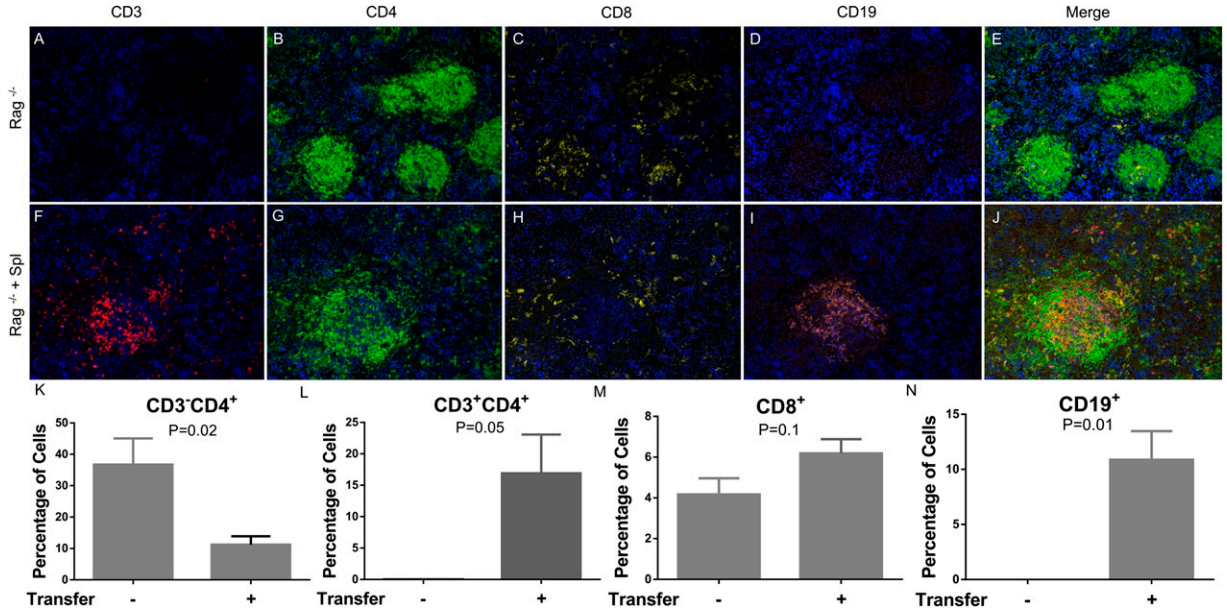

FIGURE 6. Adoptive transfer of splenocytes into Rag$^{-/-}$ mice. Ten million splenocytes from WT C57BL/6 mice were transferred into Rag1$^{-/-}$ mice. Spleens were harvested 14 d later. Multiplex fluorescent IHC was performed on Rag$^{-/-}$ mice (**A**–**E**) and adoptively transferred animals (**F**–**J**). (**K**–**N**) The percentage of positive cells was enumerated based on total DAPI^{+} cells in the area imaged. The p values were calculated using the unpaired t test (n = 3–4). Original magnification ×20.

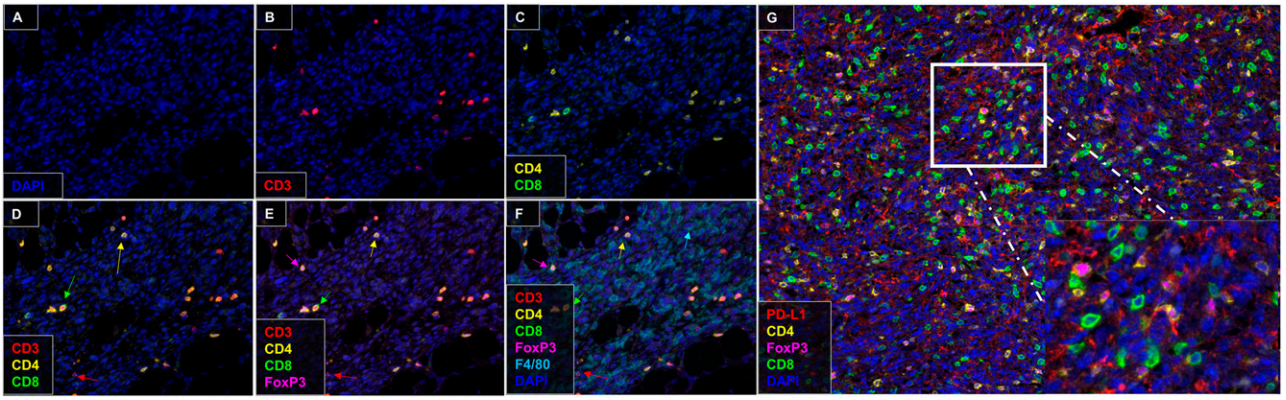

FIGURE 7. Multiplex fluorescent IHC on tumor samples. (**A**–**F**) MCA310 sarcoma tumor was stained with CD3, CD4, CD8, Foxp3, F4/80, and DAPI. Red arrows indicate $CD3^+CD4^-CD8^-$ T cells, green arrows indicate $CD3^+CD8^+$ T cells, yellow arrows indicate $CD3^+CD4^+Foxp3^-$ T cells, and magenta arrows indicate $CD3^+CD4^+Foxp3^+$ T cells. (**G**) SCCVII squamous cell carcinoma tumor was stained with PD-L1, CD4, CD8, Foxp3, and DAPI. Inset: higher-magnification view of a section of tumor demonstrating CD4, CD8, Foxp3, and PD-L1 staining. Original magnification ×20.

Fig. 1C, 1D). In addition, we had success with polyclonal Abs targeting PD-L1 (Fig. 7G) and granzyme B (Supplemental Fig. 4).

While validating the specificity of CD4 staining (Fig. 2), we observed a significant population of $CD3^-CD4^+$ cells aggregating into a follicular pattern. Because these cells appear in $Rag1^{-/-}$, pmel, and TRP1 spleens, it is possible that they reside in follicles devoid of T and B cells; alternatively, they may be instrumental in recruiting T and B cells to the follicles in the spleen. When we adoptively transferred WT splenocytes into $Rag1^{-/-}$ mice, we observed an accumulation of $CD3^+$ T cells and $CD19^+$ B cells in the vicinity of these follicles (Fig. 6D–J), suggesting that these $CD3^-CD4^+$ cells may mediate the recruitment and potential development of B cells. These findings need confirmation in future studies.

The presence of these $CD3^-CD4^+$ cells in the spleen outlines the importance of multiplex staining to reliably study various immune cell populations. We were able to apply the technique in a multiplex platform to examine multiple parameters simultaneously in fixed specimens of murine spleens (Fig. 5), as well as two orthotopically implanted tumor cell lines (Fig. 7). To study these sensitive epitopes, such as CD4 and CD8α, in a multiplex platform, a mild Ag-stripping solution, such as glycine, is superior for proper preservation of signal compared with heat-mediated Ag-stripping solution (Fig. 4). We conclude that the pH-10 stripping buffer is the optimal buffer solution for this T and B cell panel because it is able to efficiently remove the previous Ab without adversely affecting the staining profile with subsequent Abs. However, a stronger stripping solution may be needed for Abs with stronger affinity, such as F4/80 for macrophages. This can be accomplished by the addition of SDS and acidic pH, which provides a harsher environment for enhanced Ab stripping.

The ability to use this multiplex IHC platform to stain different populations of immune cells within the tumor microenvironment provides data about quantity and spatial relationships that are informative. It is also important to be able to examine the functionality of these cells, and we have begun to examine this using granzyme B expression in CD8 T cells (Supplemental Fig. 4). A limitation that we encountered is the lack of effective Abs to study cytokines expressed by these cells. Genomic approaches may be an alternative to address some of these limitations. Zinc-based fixation has not been shown to adversely affect the quality of DNA and RNA in the sample (17, 28), and we had preliminary success analyzing mRNA expression profiles in murine tumors fixed with zinc-based buffer (data not shown).

To our knowledge, our study is the first to report on the ability to perform multiplex IHC with CD4, CD8, and CD19 to identify basic T and B cell populations in zinc-fixed paraffin-embedded murine tissues. Importantly, this method provides the ability to examine the spatial interactions and relationships among multiple parameters on a single tissue section. Additionally, this approach will likely allow for additional Abs, which are traditionally reserved for flow cytometry and frozen sections, to be used on paraffin-embedded samples.

Acknowledgments

We thank Dr. Lisa Coussens for providing the spleens from CD4-knockout animals and Cliff Hoyt, Chichung Wang, and Kristin Roman (PerkinElmer) for advice on staining methods and image analysis.

Disclosures

B.A.F. is a member of PerkinElmer's Health Sciences Division, Scientific Advisory Board. The other authors have no financial conflicts of interest.

References

1. Fridman, W. H., F. Pagès, C. Sautès-Fridman, and J. Galon. 2012. The immune contexture in human tumours: impact on clinical outcome. *Nat. Rev. Cancer* 12: 298–306.
2. Herbst, R. S., J. C. Soria, M. Kowanetz, G. D. Fine, O. Hamid, M. S. Gordon, J. A. Sosman, D. F. McDermott, J. D. Powderly, S. N. Gettinger, et al. 2014. Predictive correlates of response to the anti-PD-L1 antibody MPDL3280A in cancer patients. *Nature* 515: 563–567.
3. Galon, J., A. Costes, F. Sanchez-Cabo, A. Kirilovsky, B. Mlecnik, C. Lagorce-Pagès, M. Tosolini, M. Camus, A. Berger, P. Wind, et al. 2006. Type, density, and location of immune cells within human colorectal tumors predict clinical outcome. *Science* 313: 1960–1964.
4. Stack, E. C., C. Wang, K. A. Roman, and C. C. Hoyt. 2014. Multiplexed immunohistochemistry, imaging, and quantitation: a review, with an assessment of Tyramide signal amplification, multispectral imaging and multiplex analysis. *Methods* 70: 46–58.
5. Collings, L. A., L. W. Poulter, and G. Janossy. 1984. The demonstration of cell surface antigens on T cells, B cells and accessory cells in paraffin-embedded human tissues. *J. Immunol. Methods* 75: 227–239.
6. Gendelman, H. E., T. R. Moench, O. Narayan, and D. E. Griffin. 1983. Selection of a fixative for identifying T cell subsets, B cells, and macrophages in paraffin-embedded mouse spleen. *J. Immunol. Methods* 65: 137–145.
7. Rehg, J. E., D. Bush, and J. M. Ward. 2012. The utility of immunohistochemistry for the identification of hematopoietic and lymphoid cells in normal tissues and interpretation of proliferative and inflammatory lesions of mice and rats. *Toxicol. Pathol.* 40: 345–374.
8. Whiteland, J. L., S. M. Nicholls, C. Shimeld, D. L. Easty, N. A. Williams, and T. J. Hill. 1995. Immunohistochemical detection of T-cell subsets and other leukocytes in paraffin-embedded rat and mouse tissues with monoclonal antibodies. *J. Histochem. Cytochem.* 43: 313–320.
9. Hicks, D. J., L. Johnson, S. M. Mitchell, J. Gough, W. A. Cooley, R. M. La Ragione, Y. I. Spencer, and A. Wangoo. 2006. Evaluation of zinc salt based fixatives for preserving antigenic determinants for immunohistochemical demonstration of murine immune system cell markers. *Biotech. Histochem.* 81: 23–30.

10. Beckstead, J. H. 1994. A simple technique for preservation of fixation-sensitive antigens in paraffin-embedded tissues. *J. Histochem. Cytochem.* 42: 1127–1134.
11. Steinert, E. M., J. M. Schenkel, K. A. Fraser, L. K. Beura, L. S. Manlove, B. Z. Igyártó, P. J. Southern, and D. Masopust. 2015. Quantifying Memory CD8 T Cells Reveals Regionalization of Immunosurveillance. *Cell* 161: 737–749.
12. Winter, H., H. M. Hu, C. H. Poehlein, E. Huntzicker, J. J. Osterholzer, J. Bashy, D. Lashley, B. Lowe, J. Yamada, G. Alvord, et al. 2003. Tumour-induced polarization of tumour vaccine-draining lymph node T cells to a type 1 cytokine profile predicts inherent strong immunogenicity of the tumour and correlates with therapeutic efficacy in adoptive transfer studies. *Immunology* 108: 409–419.
13. Khurana, D., E. A. Martin, J. L. Kasperbauer, B. W. O'Malley, Jr., D. R. Salomao, L. Chen, and S. E. Strome. 2001. Characterization of a spontaneously arising murine squamous cell carcinoma (SCC VII) as a prerequisite for head and neck cancer immunotherapy. *Head Neck* 23: 899–906.
14. Borowitz, M. J., B. P. Croker, and J. Burchette. 1982. Immunocytochemical detection of lymphocyte surface antigens in fixed tissue sections. *J. Histochem. Cytochem.* 30: 171–174.
15. McLean, I. W., and P. K. Nakane. 1974. Periodate-lysine-paraformaldehyde fixative. A new fixation for immunoelectron microscopy. *J. Histochem. Cytochem.* 22: 1077–1083.
16. Brenes, F., S. Harris, M. O. Paz, L. M. Petrovic, and P. J. Scheuer. 1986. PLP fixation for combined routine histology and immunocytochemistry of liver biopsies. *J. Clin. Pathol.* 39: 459–463.
17. Wester, K., A. Asplund, H. Bäckvall, P. Micke, A. Derveniece, I. Hartmane, P. U. Malmström, and F. Pontén. 2003. Zinc-based fixative improves preservation of genomic DNA and proteins in histoprocessing of human tissues. *Lab. Invest.* 83: 889–899.
18. Shortman, K., and W. R. Heath. 2010. The CD8+ dendritic cell subset. *Immunol. Rev.* 234: 18–31.
19. Kim, M. Y., F. M. McConnell, F. M. Gaspal, A. White, S. H. Glanville, V. Bekiaris, L. S. Walker, J. Caamano, E. Jenkinson, G. Anderson, and P. J. Lane. 2007. Function of CD4+CD3− cells in relation to B- and T-zone stroma in spleen. *Blood* 109: 1602–1610.
20. Kim, M. Y., S. Rossi, D. Withers, F. McConnell, K. M. Toellner, F. Gaspal, E. Jenkinson, G. Anderson, and P. J. Lane. 2008. Heterogeneity of lymphoid tissue inducer cell populations present in embryonic and adult mouse lymphoid tissues. *Immunology* 124: 166–174.
21. Vremec, D., J. Pooley, H. Hochrein, L. Wu, and K. Shortman. 2000. CD4 and CD8 expression by dendritic cell subtypes in mouse thymus and spleen. *J. Immunol.* 164: 2978–2986.
22. Feng, Z., S. Puri, T. Moudgil, W. Wood, C. C. Hoyt, C. Wang, W. J. Urba, B. D. Curti, C. B. Bifulco, and B. A. Fox. 2015. Multispectral imaging of formalin-fixed tissue predicts ability to generate tumor-infiltrating lymphocytes from melanoma. *J. Immunother. Cancer* 3: 47.
23. Esashi, E., H. Ito, K. Ishihara, T. Hirano, S. Koyasu, and A. Miyajima. 2004. Development of CD4+ macrophages from intrathymic T cell progenitors is induced by thymic epithelial cells. *J. Immunol.* 173: 4360–4367.
24. Garon, E. B., N. A. Rizvi, R. Hui, N. Leighl, A. S. Balmanoukian, J. P. Eder, A. Patnaik, C. Aggarwal, M. Gubens, L. Horn, et al. KEYNOTE-001 Investigators. 2015. Pembrolizumab for the treatment of non-small-cell lung cancer. *N. Engl. J. Med.* 372: 2018–2028.
25. Dolled-Filhart M., C. M. Roach, G. Toland, J. Musser, G. M. Lubiniecki, G. Ponto, K. Emancipator; Merck & Co., Inc., Kenilworth, NJ; Dako, North America, Carpinteria, CA; Dako North America, Inc., Carpinteria, CA. 2015. Development of a PD-L1 immunohistochemistry (IHC) assay for use as a companion diagnostic for pembrolizumab (MK-3475) in non-small cell lung cancer (NSCLC). *J. Clin. Oncol.* 33: 2015 (Suppl. abstract 11065).
26. Winter, H., N. K. van den Engel, D. Rüttinger, J. Schmidt, M. Schiller, C. H. Poehlein, F. Löhe, B. A. Fox, K. W. Jauch, R. A. Hatz, and H. M. Hu. 2007. Therapeutic T cells induce tumor-directed chemotaxis of innate immune cells through tumor-specific secretion of chemokines and stimulation of B16BL6 melanoma to secrete chemokines. *J. Transl. Med.* 5: 56.
27. Liu, J., Y. Yuan, W. Chen, J. Putra, A. A. Suriawinata, A. D. Schenk, H. E. Miller, I. Guleria, R. J. Barth, Y. H. Huang, and L. Wang. 2015. Immune-checkpoint proteins VISTA and PD-1 nonredundantly regulate murine T-cell responses. *Proc. Natl. Acad. Sci. USA* 112: 6682–6687.
28. Lykidis, D., S. Van Noorden, A. Armstrong, B. Spencer-Dene, J. Li, Z. Zhuang, and G. W. Stamp. 2007. Novel zinc-based fixative for high quality DNA, RNA and protein analysis. *Nucleic Acids Res.* 35: e85.